Reactive Compatibilization and Fracture Behavior in Nylon 6/VLDPE Blends

ANDREA LAZZERI,[1]* MARCO MALANIMA,[1] MARIANO PRACELLA[2]

[1] Center for Materials Engineering, University of Pisa, Via Diotisalvi 2, 56126 Pisa, Italy

[2] Study Center for Polyphasic and Biocompatible Macromolecular Materials, CNR, Via Diotisalvi 2, 56126 Pisa, Italy

Received 2 March 1999; accepted 27 May 1999

ABSTRACT: A physical and mechanical characterization of blends of Nylon 6 (PA6) and very low density polyethylene (VLDPE), functionalized with maleic anhydride (MA) or diethylmaleate (DEM) is reported. The functionalization of VLDPE with MA and DEM was performed by reactive extrusion in a twin-screw (Berstoff) extruder in the presence of dicumylperoxide. The PA6/VLDPE, PA6/VLDPE-*g*-MA, and PA6/VLDPE-*g*-DEM blends with composition ratio of 80 : 20 (wt %) were obtained by using a twin-screw Werner & Pfleiderer extruder. An industrial-type blend based on PA6 and MA-grafted ultra low density polyethylene (ULDPE-*g*-MA) was also tested for comparison. All blends were then characterized by optical and scanning electron microscopy, differential scanning calorimetry, and dynamic mechanical thermal analysis. The results of slow fracture and impact tests showed that the ductile-brittle transition temperature of the examined blends depends on the type of functional group and test speed. © 1999 John Wiley & Sons, Inc. J Appl Polym Sci 74: 3455–3468, 1999

Key words: reactive extrusion; blends; fracture toughness; interparticle distance; functional group reactivity

INTRODUCTION

Polyolefins are often blended to nylons for improving some polyamide properties, particularly their toughness. The use of polyolefins functionalized with reactive groups such as carboxyl derivatives has been reported in the literature as a suitable method for promoting the compatibilization of the polyamide matrix with the dispersed polyolefin phase.[1,2] The presence of carboxyl or anhydride groups grafted on the polyolefin chains during melt blending can give rise to interfacial reactions with the amine or amide groups of the polyamide, leading to the formation of *in situ* copolymers which contribute to decrease the interfacial tension and to enhance phase dispersion and interfacial adhesion between the polymer components.[1,3]

To improve the impact resistance of polyamides, various elastomeric polymers containing acrylates (butyl acrylate, ethyl acrylate, methyl methacrylate, etc.), acrylic acid (AA), or maleic anhydride (MA) have been blended in the melt with Nylon 6 (PA6) and Nylon 6,6 (PA66).[1] The effect of an ethylene-propylene/PA6 graft copolymer, formed during melt blending of carboxyl or anhydride modified ethylene-propylene copolymers and PA6, on the morphology and mechanical properties of the blends has been extensively examined.[4] Diethylmaleate (DEM) has been proposed as an alternative to maleic anhydride as a grafting moiety for polyethylene (PE).[5]

* Currently on leave: c/o Massachusetts Institute of Technologies, Department of Mechanical Engineering, 77 Massachusetts Avenue, Cambridge, MA 02139, USA.

Correspondence to: A. Lazzeri.

Journal of Applied Polymer Science, Vol. 74, 3455–3468 (1999)
 CCC 0021-8995/99/143455-14

There is also a growing interest in this type of blend because of recycling of postconsumer scrap materials based on polyamide and polyolefins.

Reactive extrusion offers the possibility of performing both the functional modification of the polyolefin and the reactive mixing with other polymer components. In particular, the chemical modification of thermoplastics in twin-screw extruders gained a lot of attention in recent years as an advantageous route for the production of new materials.

The mechanism and the control of free radical grafting reactions of polyolefins with MA or glycidyl methacrylate (GMA) in the melt[6–8] has been analyzed under different conditions. The effect of extrusion on the grafting of PE of various density with DEM has also been described.[9]

However, only a few experimental data have been reported so far concerning the relationships between morphology and fracture resistance of these blends. In fact, the size of the dispersed particles represents a critical factor in controlling the fracture toughness, or more correctly the *interparticle distance*, which is lower as the particle size decreases or as the volume fraction of the dispersed phase increases. It has been shown that a critical value of this parameter exists above which a transition from a ductile to brittle behavior occurs in impact tests.[10–13]

In the present report we consider the effect of the addition of very low density polyethylene (VLDPE), functionalized with DEM or MA in blends with PA6, obtained by reactive extrusion. The main aim is to investigate the effect of the functional groups on the morphological, thermal, and mechanical properties of the blends, with a particular attention to the relationships between phase dispersion and fracture properties.

EXPERIMENTAL

Materials

Commercial samples of PA6 and VLDPE were used in this work. PA6 (ADS 40), with a molecular weight of 62.0 kg/mol, relative viscosity 3.8 (measured in sulfuric acid with a purity of 96%), and NH_2 content of 32 meq/kg, was kindly supplied by Nyltech (Milano, Italy). VLDPE was a product by Polimeri Europa (Milano, Italy), with a density of 885.6 kg/m^3, melt flow index, MFI = 1.77 g/(10 min), and comonomer ratio C3/C4 = 9 : 4. All polymers were carefully dried under vacuum before use.

VLDPE Functionalization

The functionalization reaction of VLDPE with DEM and MA was performed in a Berstoff (Florence, KY) ECS-2E25 twin-screw extruder (screw diameter: 25 mm, length: 905 mm), using a rotation speed of 35 rpm. DCP with 98% purity, produced by Aldrich Chemicals (Milwaukee, WI), was used in both cases as radical initiator.

The grafting of VLDPE with DEM (VLDPE-*g*-DEM) was obtained by using a total amount of 10 pph DEM (Aldrich Chemicals), in two separate passages in the extruder, according to the procedure described in Rosales et al.[9] In the first stage, 8 pph DEM and VLDPE were premixed at 150°C. Then, in the second stage, DCP was added with the remaining DEM to the mixture obtained in the first passage to start the grafting reaction, which was performed using a temperature profile 110/130/145/145/150/150/150°C. The extruded material was cooled in a water bath and pelletized. The resulting VLDPE-*g*-DEM contained 0.43 mol % of diethylmaleate.

The functionalization of VLDPE with MA (VLDPE-*g*-MA) was performed in a single extrusion process by mixing the polyolefin and MA, with a composition ratio of 95 : 5, adding the DCP initiator through a secondary port in the last section of the extruder. The reaction was performed at 35 rpm with a temperature profile of 130/155/160/175/180/180/180°C. The VLDPE-*g*-MA copolymer contained 0.8 pph MA.

The functionalized products were washed carefully with acetone and dried under vacuum at 60°C for 8 h. The grafting degree of the VLDPE-*g*-DEM sample was determined by Fourier transform infrared (FTIR) and ^{1}H-nuclear magnetic resonance (NMR) calibration curves,[9] whereas the grafting degree of the VLDPE-*g*-MA was obtained by titration of the carboxyl groups with KOH in an alcoholic solution.

Blending

Blends of PA6 with VLDPE, VLDPE-*g*-DEM, and VLDPE-*g*-MA with a composition ratio of 80 : 20 w/w were prepared by means of a Werner & Pfleiderer (Ramsey, NJ) ZSK-30 twin-screw extruder (screw diameter: 30 mm, length: 706 mm) with a temperature profile of 170/210/235/230/220°C and rotating speed of 110 rpm. Pure PA6 was also

passed into the extruder to compare materials with the same thermomechanical history.

An industrial type blend, consisting of PA6 and ULDPE grafted with approximately 0.5 pph MA and having a composition ratio of 80 : 20 w/w, supplied by Nyltech, was also used for a comparison. This material was extruded in the Werner & Pfleiderer extruder under the same conditions as the other blends. After extrusion, all blends were pelletized.

Moulding

To prepare samples for the mechanical characterization, the blends were molded both by vacuum-bag (VB) compression and injection molding. In the latter case, a Sandretto injection molding machine was used.

The VB compression molding technique, was investigated, in the first part of this work, to avoid both orientation of the materials during injection molding and, at the same time, to prevent oxidative degradation of the PA6 matrix during compression molding. For this purpose, the mold was encapsulated into an especially prepared Mylar bag and vacuum was applied inside the bag before heating the sample in a conventional molding machine. All blends were VB compression molded in rectangular plaques of 3, 7, and 10 mm thickness. For the plain PA6 and the homopolymer blend, the molding temperature used was 230°C, whereas blends with functionalized VLDPE were molded at temperatures in the range of 240–250°C, depending on the thickness of the plaques.

All the VB compression-molded samples appeared whiter in color than the injection-molded samples, thus indicating a lower degree of oxidative degradation and homogeneous under both the optical and scanning electron microscopes (SEM). Under a preliminary fracture mechanics analysis, however, an anomalous behavior was shown by the blends with functionalized polyolefin. In fact, whereas cracks propagating in plain PA6 and PA6/VLDPE VB compression-molded samples presented a regular lenticular shape,[14] due to slower propagation near the surface of the specimen, in the case of VB compression-molded samples of PA6/VLDPE-*g*-DEM and PA6/VLDPE-*g*-MA, crack propagation was completely irregular. On the other hand, injection-molded samples of the same blends with functionalized polyolefin, did not present any anomaly in crack propagation.

This preliminary work indicated that VB compression molding is unsuitable for preparing samples of blends with functionalized VLDPE, probably due to insufficient shear of the material in the mold, and was abandoned. In the remainder of the article, only results obtained on injection molded samples will be reported.

FTIR

Films of VLDPE-*g*-DEM were analyzed by means of a Perkin-Elmer 1750 FTIR spectrophotometer with a resolution of 2 cm^{-1}. The absorbance of the band at 1740 cm^{-1}, characteristic of the stretching of carbonyl groups, and the bands at 1460 and 720–730 cm^{-1}, characteristic of methyl and methylene groups, were used for the evaluation of the grafting degree of DEM on the VLDPE. The peak area ratios 1740 : 1460 and 1740 : (720 + 730) were used for the correlations with the grafting degree determined by ^{1}H-NMR.[9]

Microscopy

A Jeol T300 SEM was used to analyze the fracture surfaces of the various samples. Blend specimens were examined under three different conditions: undeformed, tested in tension, and in fracture experiments.

In the first case, the samples were broken at liquid nitrogen temperature to show the morphology of the dispersed phase. In the second case, samples were cut out of the gauge length of specimens, previously tested in tension until break, a crack was initiated by means of a saw notch, followed by a razor cut, and subsequently broken at liquid nitrogen temperature to show the effects of deformation.

In the third case, the fracture surface of samples broken at different temperatures in slow bending and in impact tests was examined.

Optical microscopy of thin sections of injection-molded samples, prepared with a Reichert–Jung 2040 microtome, was also performed using a Leitz Ortolux model II-POL BK microscope.

Calorimetric Analysis

A Perkin–Elmer differential scanning calorimetry (DSC)-2C calorimeter equipped with Data Station 3600, was used to analyze samples cut from pellets. All measurements were performed under nitrogen flow. The temperature calibration of DSC was obtained by measuring the melting

temperature of standard (indium and azobenzole).

The thermograms were recorded, on a first run, from room temperature to the melting of the sample, at a heating rate of 10°C/min, then on the successive cooling at the same rate of 10°C/min. A second heating run was then performed at 10°C/min. The glass transition temperature was determined from the onset of the transition as the intercept between the recorded slope and the baseline of the instrument, and at the middle point of the transition. Temperature and heats of crystallization/melting were determined from the peak maxima and the corresponding areas in the thermograms, respectively.

Mechanical Properties

Specimens for mechanical analysis were cut from injection-molded thick rectangular plaques, size 195 × 117 × 6 mm (see Molding section above). Before testing, all materials were kept in a desiccator to maintain them in a dry-as-molded condition.

Tensile tests were performed with an Instron 1185 tensometer, on (VB) compression-molded and injection-molded samples according to ASTM D 638-82. All tests were performed at a crosshead speed of 5 mm/min.

Dynamical-Mechanical Properties

Dynamical-mechanical analysis was performed with a Polymer Laboratories DMTA-I, at a frequency of 1 Hz, on samples with a size of 20 × 10 × 1 mm cut from the molded plaques. The temperature range scanned was from −100 to 220°C, and the scan speed was 4°C/min.

Fracture Mechanics

The fracture resistance of the blends was studied using the J-integral approach.[14] This method enables measurement of the resistance of a polymer to fracture initiation by a multispecimen technique that uses a series of specimens with a deep and sharp notch of the same initial length, a, according to the ESIS protocol.[15]

Each specimen is loaded until some crack propagation occurs. At this point, the test is stopped and an iodine solution is poured into the open crack tip, so that the resulting staining reveals, after a subsequent breakage at low temperature or in impact, the crack growth, Δa, on the surface. The energy up to the displacement at which the test is stopped, U, is then measured and J is calculated from:

$$J = \frac{2U}{B(W - a)}$$

where W is the width of the sample and B its thickness, which for these tests were 20 and 6 mm, respectively. The initial crack length was 10 mm. Each specimen was loaded to different levels to obtain a series of Δa values.

The critical J_{IC} is defined as the limit of J for $\Delta a \rightarrow 0$, so that J_{IC} can be determined by plotting of J vs Δa. The experimental points lie on a line that is called the R-curve. A correction for the apparent crack growth due to blunting of the crack tip, Δa_b, is necessary and this can be done by considering that:

$$J = 2\sigma_y \Delta a_b$$

where σ_y is the yield stress. Plotting this expression on the $J - \Delta a$ curve gives the so-called blunting line. J_{IC} is then taken as the intercept of the blunting line with the R-curve. The slope of the R-curve, dJ/da, is an important parameter which gives us a measure of the resistance to crack propagation.

On materials showing brittle behavior in notched fracture tests, the critical strain energy release rate, G_{IC}, was used to measure fracture toughness, according to ASTM D5045.[16]

All tests were performed at a speed of 5 mm/min with an Instron tensometer model 1185.

Impact and 3-Point Bending Testing

Other fracture tests were performed in the 3-Point Bending (3PB) configuration both in slow bending and in impact tests, at different temperatures, on sharply notched specimens, size 115 × 17.5 × 6 mm, and an initial crack length of 9 mm to explore the effect of test speed, in the same geometrical configuration. In both cases, the span used was 70 mm whereas test speeds were 5 mm/min and 3.9 m/s, respectively. In these tests, the crack is propagated through the sample until final separation. The Charpy test was conducted on a CEAST MK2 impact pendulum (CEAST, Torino, Italy).

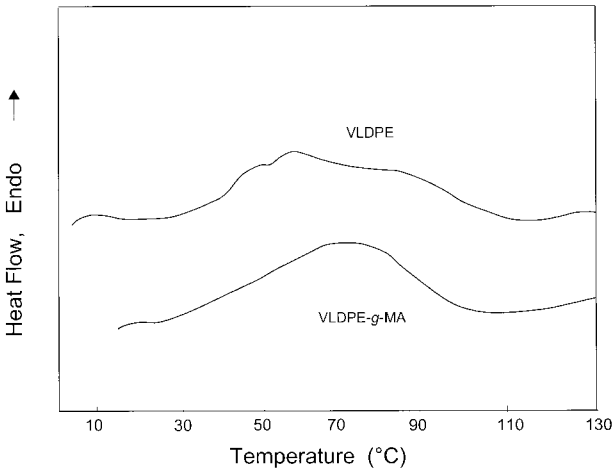

Figure 1 Melting thermograms of plain VLDPE (first and second heating run).

RESULTS

Thermal Behavior

The DSC melting thermograms of plain VLDPE and VLDPE-*g*-MA, recorded on the first and second heating runs, are shown in Figures 1 and 2.

The melting behavior (first run) of the extruded polyolefin samples is clearly affected by the presence of the MA functional group. VLDPE displays a multiple endotherm with main peaks at about 57°C and 85°C, which seems to be ascribed to polymer fractions with a different degree of chain branching. For this sample, a crystallinity value of approximately 10% was calculated from melting enthalpy measurements. VLDPE-*g*-MA showed a single very broad peak centered at approximately 69°C. On the second run, after cooling from the melt at 10°C/min, both samples presented a broad melting curve with maximum at approximately 70°C. However, the melting enthalpy of VLDPE (39.5 J/g) results were larger than that of VLDPE-*g*-MA (24.3 J/g), indicating a lower degree of crystallinity for the functionalized polyolefin.

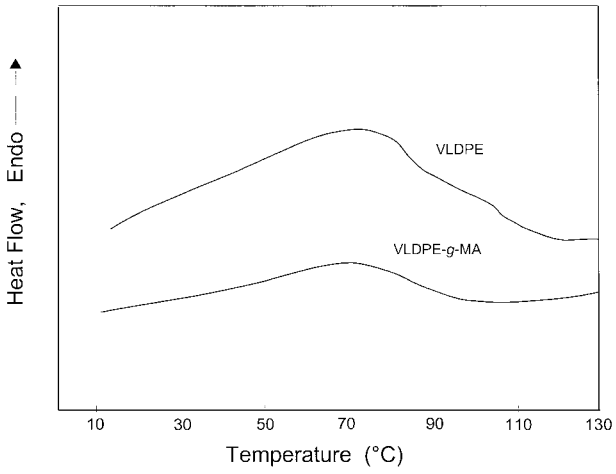

Figure 2 Melting thermograms of plain VLDPE-*g*-MA (first and second heating run).

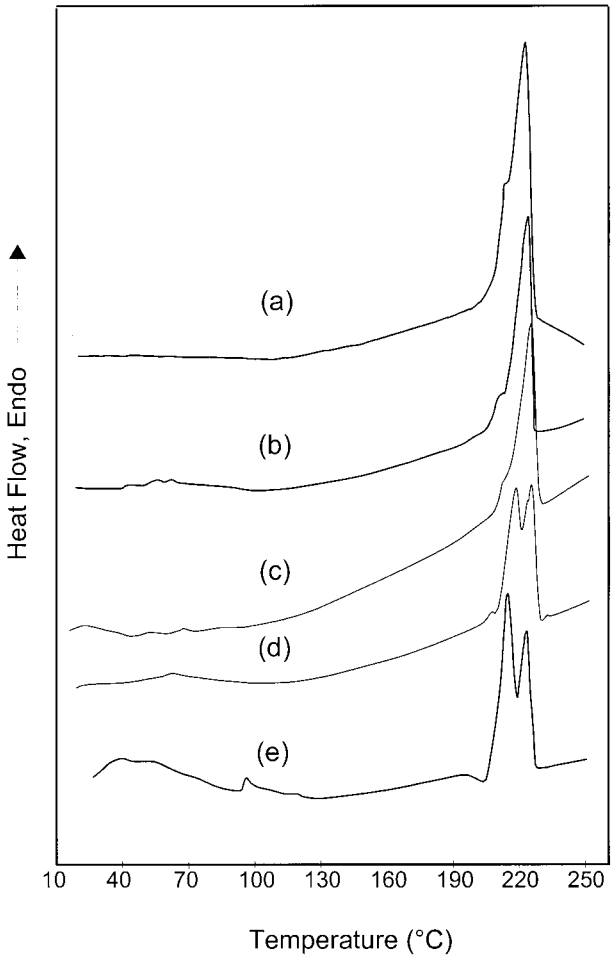

Figure 3 First run melting thermograms of plain PA6 (a) and blends PA6/VLDPE (b), PA6/VLDPE-*g*-DEM (c), PA6/VLDPE-*g*-MA (d), and Nyltech (e).

The melting thermograms of plain PA6 and various blends are reported in Figures 3 and 4 for the first and second run, respectively. The blends display melting endotherm characteristics of the polyolefin component, in the range of 50–85°C, and of the polyamide, in the range of 190–220°C. For PA6, multiple melting peaks are usually observed as a consequence of melting and recrystallization phenomena during heating and depend on the presence of polymorphic crystal modifica-

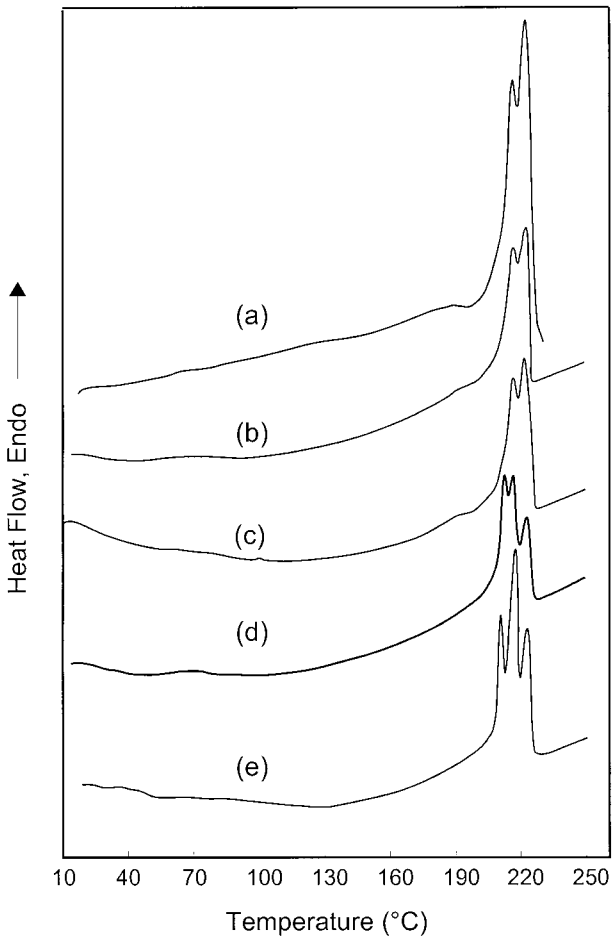

Figure 4 Second run melting thermograms of plain PA6 (a) and blends PA6/VLDPE (b), PA6/VLDPE-*g*-DEM (c), PA6/VLDPE-*g*-MA (d), and Nyltech (e).

tions.[17] The highest melting peak (220°C) is referred to PA6 crystals (α-form) which have reorganized during the heating run, whereas the lower peak at approximately 210°C corresponds to the crystals formed on cooling from the melt. The intensity and position of the latter peak depend on the crystallization conditions of the sample, and generally increase with increasing the crystallization temperature (under isothermal conditions) or by decreasing the crystallization rate.

From Figure 3, it can be observed that the blend PA6/VLDPE-*g*-DEM displays a melting behavior of the polyamide phase similar to that of the homopolymers blend PA6/VLDPE and of plain PA6, with a melting peak above 220°C and a shoulder at about 210°C. On the other hand, PA6/VLDPE-*g*-MA and the Nyltech blend show two sharp melting peaks at about 215°C and 222°C. On cooling from the melt, all blends present a very similar crystallization behavior with a single sharp exotherm in the range of 185–189°C. On the second heating run (Fig. 4), the blends PA6/VLDPE and PA6/VLDPE-*g*-DEM show a double melting peak at temperatures near those of plain PA6 (approximately 216°C and 222°C), whereas the blends containing the MA functionalized polyolefin present a third intense melting peak at a temperature below 210°C. This additional peak at a lower melting temperature can be ascribed to a fraction of PA6 crystals which have a different thermal stability, most likely those characteristic of the polymorphic γ-form. In fact, these crystals, which are preferentially formed on cooling at temperatures below 180°C, have a melting temperature close to 210°C.[17]

The presence of γ-form crystals can be correlated with the occurrence of interfacial interactions between the polyamide and the functionalized polyolefin phase. It has been shown for blends of PA6 and polyolefins (PE, PP) modified with AA[18] that the fraction of γ-form crystals, as measured by WAXS analysis, increases with the functionalized polyolefin content and is much higher than that observed for the blends of homopolymers obtained under the same crystallization conditions. This effect has been associated with the dispersion degree of the components in the blend, which can markedly affect the crystal nucleation phenomena in the melt.[19,20]

The differences observed in the melting behavior of the blends PA6/VLDPE-*g*-DEM and PA6/VLDPE-*g*-MA seem to be accounted for by a different degree of phase interactions in these systems, likely due to a higher reactivity of MA groups of the latter toward the amide and amino end groups of the polyamide, determining a larger phase dispersion and interfacial adhesion between the blend components, as supported by the morphological analysis of the fracture surfaces.

The values of the peak temperatures of the polyamide, and the relevant enthalpies of transition, recorded both on the heating and cooling runs, are summarized for the various examined blends in Table I. By comparing the melting (and crystallization) enthalpies of the PA6 phase in the various blends, it appears that the crystallinity degree of the polyamide, in the compatibilized systems, is generally lower than for plain PA6 and for the homopolymer blend PA6/VLDPE. The glass transition temperature remains almost unchanged for all blends (about 50°C) with a lower value than that observed for the plain PA6 (56°C).

Table I Calorimetric Data

	First Heating		Cooling		Second Heating		
	T_m (°C)	ΔH_m (J/g)	T_c (°C)	ΔH_c (J/g)	T_m (°C)	ΔH_m (J/g)	T_g (°C)
PA6	220.8	59.9	179.9	−56.8	220.0	68.9	56.0
PA6/VLDPE	222.7	46.8	188.9	−50.3	221.7	52.6	49.5
PA6/VLDPE-*g*-DEM	223.2	43.7	188.2	−52.9	221.7	49.5	50.4
PA6/VLDPE-*g*-MA	222.3	46.1	188.5	−47.4	222.4	46.1	49.7
Nyltech	222.2	46.4	189.2	−48.2	222.8	50.3	49.8

DMTA Analysis

Plots of the dynamic modulus and tan δ as a function of temperature are shown in Figure 5 for PA6 and blends. For plain PA6, the main transitions (tan δ peaks) are observed respectively at approximately −60°C (β relaxation) and 52°C (α relaxation). The latter, corresponding to the glass transition, is preceded by a marked shoulder at approximately 25°C. Another characteristic transition of PA6 at lower temperature, approximately −100°C (γ relaxation), is not evidenced in the plot. The blends display a marked tan δ peak near 70°C, corresponding to the α relaxation of PA6, and a minor one at approximately −30°C, which is to be ascribed to the glass transition (α relaxation) of the polyolefin component. Only in the case of the homopolymer blend PA6/VLDPE, a shoulder is observed at approximately 25°C in the region between the two main transitions. Such a peak, similar to that observed for the plain PA6 sample, can be associated with the presence of water in these samples.[21]

Microscopy

Scanning electron microscopy was performed on all materials, in three different conditions: undeformed, tested in tension, and in impact.

Undeformed Samples

Figure 6 shows a micrograph of the cold fractured surface of an injection-molded sample of PA6/

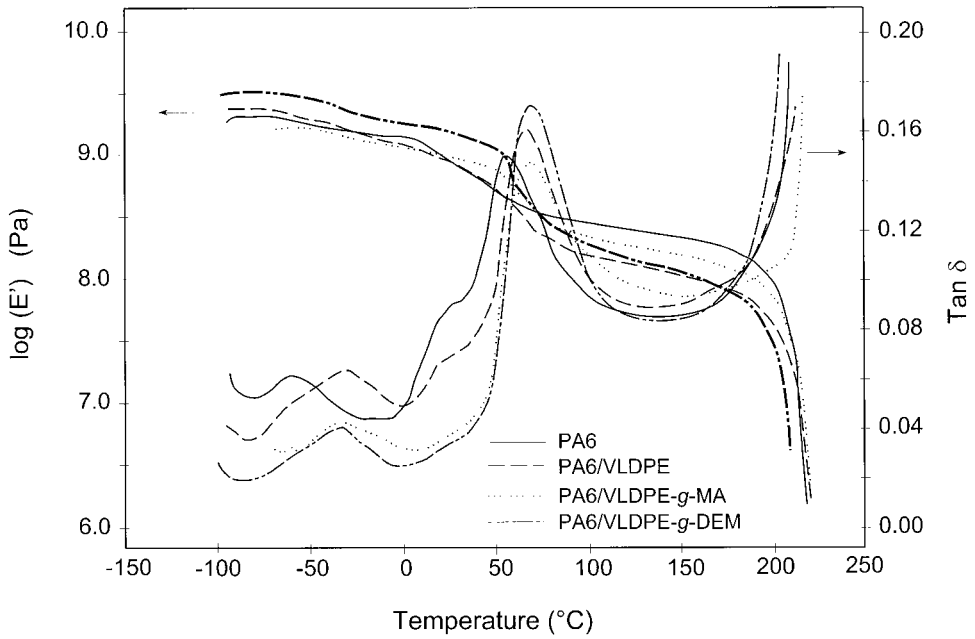

Figure 5 Elastic and loss moduli as a function of temperature for PA6 and its blends with VLDPE.

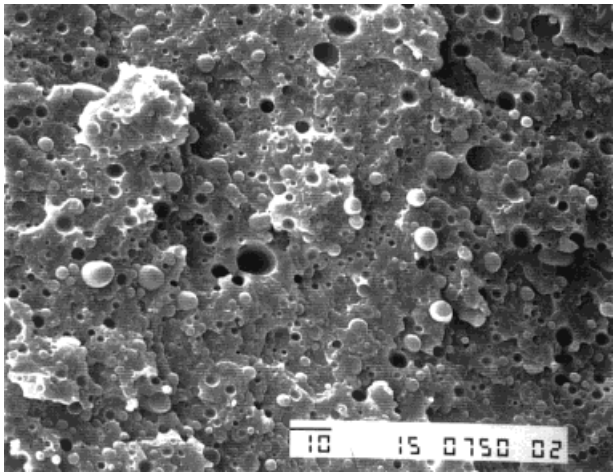

Figure 6 Micrograph of the cold fractured surface of an injection-molded sample of PA6/VLDPE (homopolymer blend).

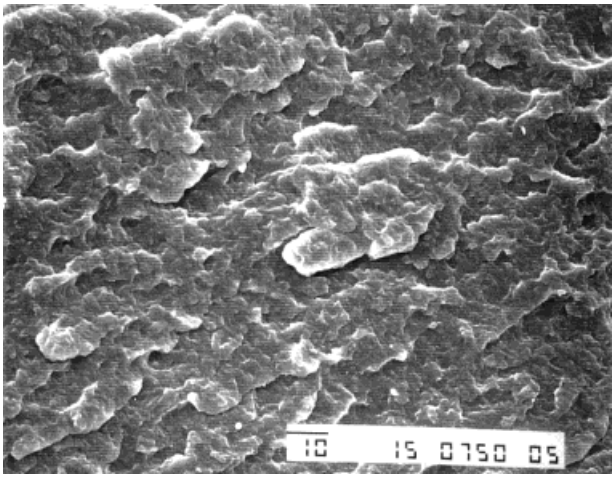

Figure 7 Micrographs of the cold fractured surface of blend PA6/VLDPE-*g*-MA.

VLDPE. The two phases are clearly visible, the polyamide being the matrix and the polyolefin the dispersed phase, in the form of approximately spherical particles. Holes, left by particles expelled during fracture, are also evident. The uncompatibilized blend appears to have a morphology that varies within the sample thickness. The average particle size is about 5 μm with bigger particles measuring approximately 8–9 μm. The particles remaining on the fracture surface are clean, thus indicating a low adhesion between the two phases.

Micrographs taken on samples of blends with functionalized VLDPE do not clearly show evidence of a two-phase morphology at magnifications accessible by the microscope. As an example, Figure 7 shows the cold fractured surface of blend PA6/VLDPE-*g*-MA.

Samples Tested in Tension

Whereas polyolefin particles observed on a cold fractured surface of specimens of PA6/VLDPE, previously drawn in a tensile test, appear elongated along the stretch direction, with clear evidence of poor adhesion between the two phases, the blends with functionalized polyolefin show a very different morphology. Figures 8–10 show the cold fractured surfaces of the PA6/VLDPE-*g*-DEM, PA6/VLDPE-*g*-MA, and Nyltech blends, respectively. In these micrographs, elongated voids, probably due to cavitation within the polyolefin phase or to debonding of the interface, are clearly visible and appear to be organized in *dilatational bands*.[22] From the ratio between the maximum and the minimum length of the voids, in the case of blend PA6/VLDPE-*g*-DEM, an approximated plastic strain of approximately 150% can be calculated whereas for PA6/VLDPE-*g*-MA and the Nyltech blends, a value of approximately 400% can be measured. All values well exceed the elongations at break of these materials. This is not surprising, because the occurrence of voids is generally accompanied by a strong inhomogeneity of plastic deformation, which tends to concentrate within dilatational bands, whereas the rest of the material may remain in the elastic state.

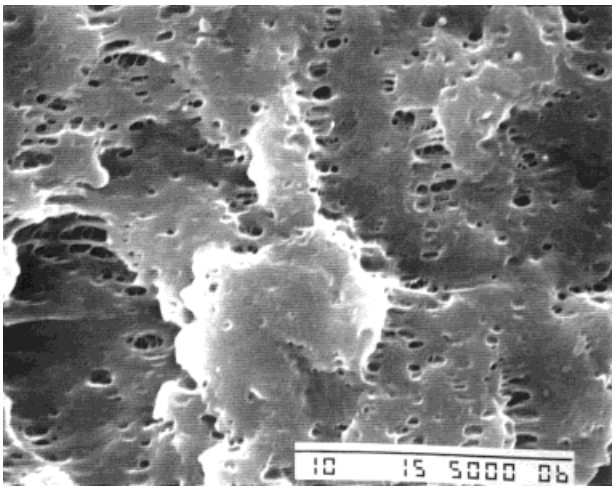

Figure 8 Micrographs of the surface of a specimen of PA6/VLDPE-*g*-DEM, previously tested in tension, and cold fractured along the draw direction.

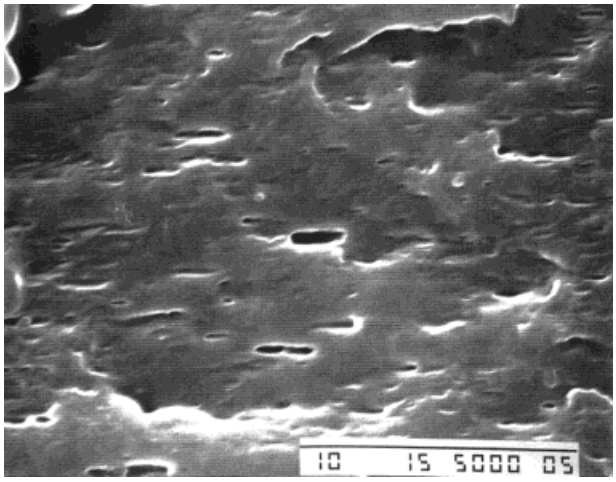

Figure 9 Micrographs of the surface of a specimen of PA6/VLDPE-*g*-MA, previously tested in tension, and cold fractured along the draw direction.

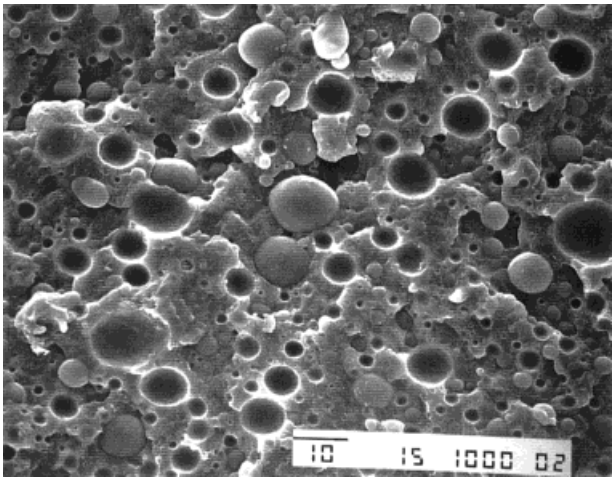

Figure 11 Fracture surface of a specimen of PA6/VLDPE (homopolymer blend) tested in impact at 40°C.

Fracture Surfaces

The fracture surface of a specimen of blend PA6/VLDPE tested in impact at 40°C, is shown in Figure 11. No sign of ductility is evident in the micrograph, and the morphology is similar to that shown by the fracture surface of undeformed samples (Fig. 6).

The fracture surface of the PA6/VLDPE-*g*-DEM blend (Fig. 12) present a very different morphology, with signs of massive cavitation phenomena taking place during crack propagation. Many voids are visible, most of which contain a particle rather being well bonded to the matrix. From these observations it may be concluded that a debonding at the matrix-particle interface has occurred followed by extensive plastic flow of the matrix around voids. Voids are also present in the case of the Nyltech (Fig. 13), and of the PA6/VLDPE-*g*-MA blends (Fig. 14), although in this case, voids seem to originate from cavitation within the polyolefin phase. The amount of voids is larger for the Nyltech blend.

The difference in the morphology of DEM and MA modified blends can be explained in terms of the different reactivity of the two grafting agents toward the nylon matrix. DEM seems not to give rise to a strong interface reaction, so its action is mainly to control the surface tension of the poly-

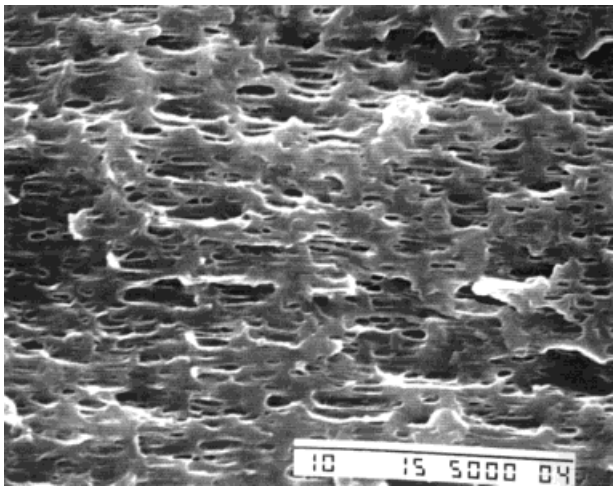

Figure 10 Micrographs of the surface of a specimen of Nyltech blend, previously tested in tension, and cold fractured along the draw direction.

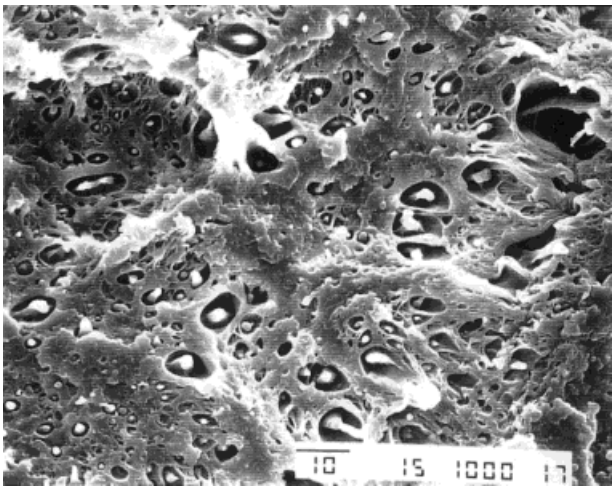

Figure 12 Fracture surface of a specimen of blend PA6/VLDPE-*g*-DEM tested in impact at 40°C.

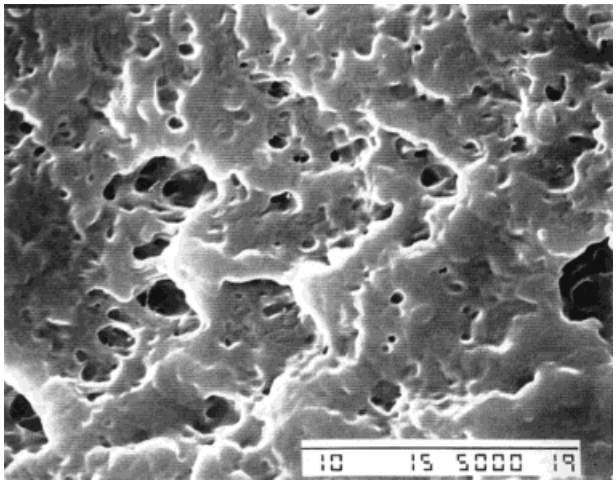

Figure 13 Fracture surface of a specimen of Nyltech blend tested in impact at 40°C.

olefin phase reducing particle size as compared with the uncompatibilized blend. As a consequence, the interface is relatively weak and cavitation mainly occurs by debonding. On the contrary, the MA functional group is likely more reactive toward the amino end groups of the nylon chains. This leads to a stronger interface and to cavitation inside the polyolefin particles.

In both blends functionalized with MA, the fracture surface does not show any evidence of fibrillation phenomena typical, for example of rubber toughened PA66[21] and is more similar to that reported for PA6 rubber blends.[23] The absence of signs of fibrillation has been attributed to the formation of a melt layer during crack propagation followed by matrix relaxation.[23]

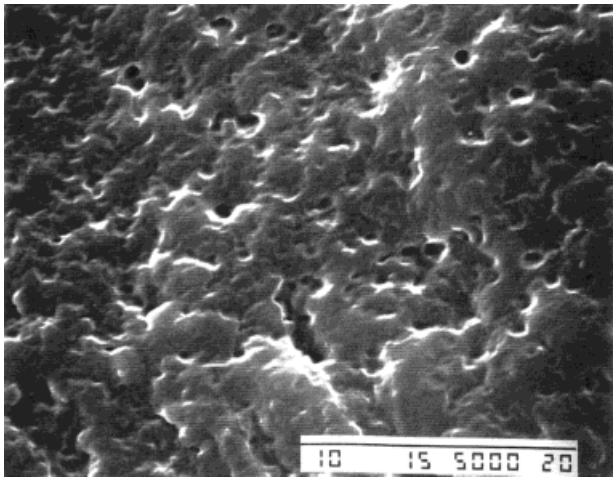

Figure 14 Fracture surface of a specimen of blend PA6/VLDPE-*g*-MA tested in impact at 40°C.

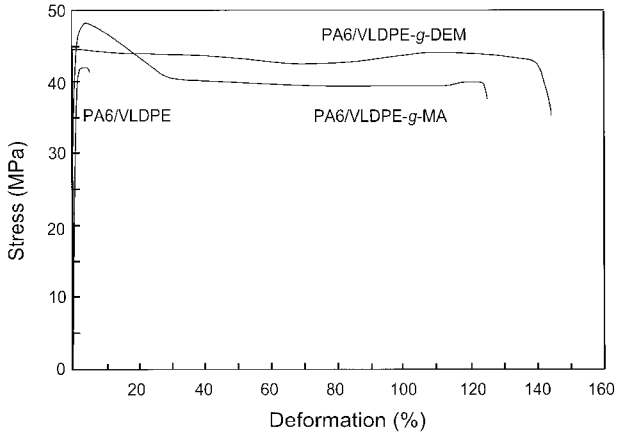

Figure 15 Stress curves for various PA6/VLDPE blends.

Fracture surfaces of samples broken at 60°C show similar features to those reported above.

Optical microscopy failed to give indications about the particle size of the blends with the exception of the PA6/VLDPE homopolymer blend in which the average particle size appeared to be approximately 5 μm. For the other materials, the particle size was below the resolution of the optical microscope.

Tensile Tests

As can be observed from Figure 15, both DEM and MA have a positive effect on the tensile properties of the blends, the unmodified blend showing very poor properties. Table II shows the main tensile parameters for these materials.

The elastic moduli and yield stresses are similar for all materials, whereas a large difference was observed in the case of the elongation at break. For the functionalized materials, the elongation at break was in the range of 120–145%, whereas the homopolymer blend was only 5%. Electron microscopy showed a rather large particle size for this blend and no adhesion between the two phases. As a consequence, during the

Table II Elastic Modulus and Yield Stress

Blend	E (GPa)	σ_y (MPa)
PA6/VLDPE	1.93	42
PA6/VLDPE-*g*-DEM	1.85	43
PA6/VLDPE-*g*-MA	2.03	47
Nyltech	1.93	45

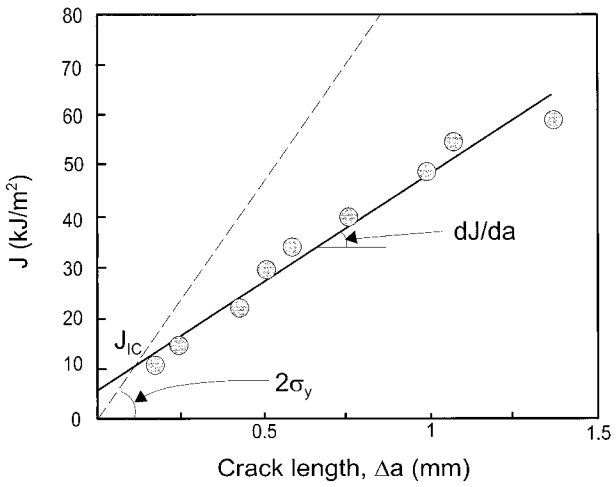

Figure 16 J versus Δa plot for blend PA6/VLDPE-*g*-MA.

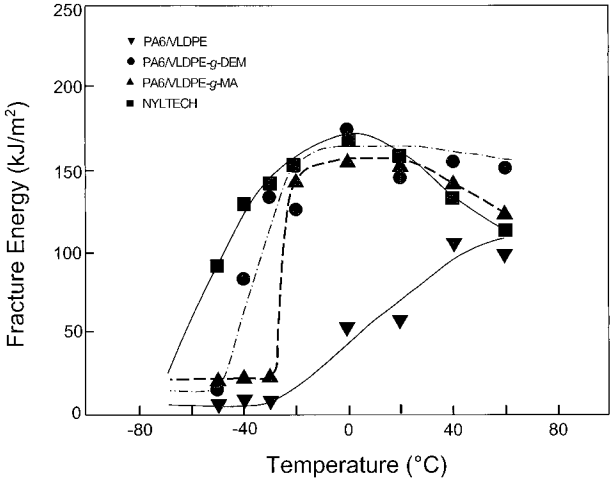

Figure 17 Total fracture energy as a function of temperature for PA/VLDPE blends, in slow speed 3PB tests.

early stages of deformation, debonding at the interface occurs with the formation of large voids which act as critical defects leading to premature fracture of the material.

Fracture Tests

Figure 16 shows a typical $J - \Delta a$ plot and Table III shows a summary of the fracture properties of the various blends. The homopolymer blend again shows a poor mechanical behavior, compared with the compatibilized blends, with a low value of both J_{IC} and dJ/da. This blend, however, has superior fracture behavior than the original PA6. This material, in fact, is brittle when tested in 3PB, and a value of 1.09 kJ/m^2 was measured for its G_{IC}, whereas when tested after being extruded, in the same conditions of the other blends, its G_{IC} falls at 0.95 kJ/m^2. Therefore, the addition of the polyolefin phase, even without a grafting agent, has resulted in a 3 times increase in the resistance to crack initiation and in a transition from a brittle to a moderately ductile behavior.

Table III Fracture Mechanics Parameters

Blend	J_{IC} (kJ/m^2)	dJ/da (MJ/m^3)
PA6/VLDPE	3	22.5
PA6/VLDPE-*g*-DEM	7.5	37
PA6/VLDPE-*g*-MA	11	41.5
Nyltech	5	54.5
Pure PA6	0.95	—

Among the compatibilized blends, the Nyltech blend has a lower crack initiation resistance, J_{IC}, but the highest dJ/da. The PA6/VLDPE-*g*-DEM blend shows intermediate J_{IC}, but a considerably lower resistance to crack propagation.

Figures 17 and 18 show the effect of temperature on the total fracture energy for this series of blends, as measured in 3PB tests. In these graphs is reported the energy necessary to fully fracture the specimen as a function of test temperature. At low speed (Fig. 17), the unfunctionalized blends show a relatively fragile behavior, especially at low temperatures, in contrast with the grafted materials. The latter blends show a sharp ductile

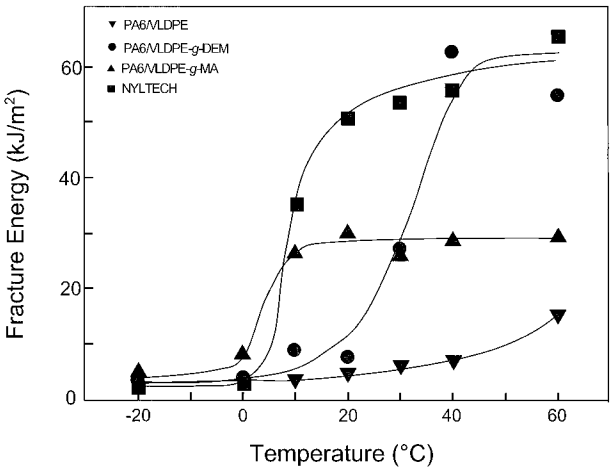

Figure 18 Total fracture energy as a function of temperature for PA/VLDPE blends, in 3PB tests in impact.

to ductile-brittle transition at a temperature located at approximately −40°C irrespective of the type of blend.

The situation changes markedly when considering tests in impact (Fig. 18). In this case, whereas the homopolymer blend still shows a brittle behavior at all test temperatures, the functionalized blends display a different value of the ductile-brittle transition temperature (DBTT) for each material. The maximum absorbed energy is also different for the Nyltech and the DEM functionalized blend showing the highest value of approximately 60 kJ/m^2. Despite this similarity, the Nyltech blend shows the best behavior, because it also has a low DBTT (5–10°C). The limited energy absorption of blend PA6/VLDPE-*g*-MA (30 kJ/m^2) is probably due to matrix degradation caused by the relatively high content of MA used in the functionalization stage.

DISCUSSION

By analyzing the fracture surface of the materials which fail in a ductile manner, we found a strong evidence for cavitation (void formation) inside the polyolefin phase or at the interface. These dilatational processes strongly enhance yielding and flow near the crack tip.[22] At slow speed all materials are able to cavitate before the crack propagates through the sample. The maximum energy absorbed is proportional to the volume of the plastic zone which is almost the same for all the functionalized blends because the phase composition is identical. The situation changes in impact. In this case, the average size of the polyolefin particles becomes important. It has been proposed that a critical interparticle distance exists, above which the material behaves in a brittle way.[10] Argon and coworkers[24–28] recently related the critical interparticle ligament thickness with the preferred orientation of the low shear resistance slip planes of lamellae parallel to the rubber-matrix interface. The lowering of the local plastic shear resistance in the interparticle ligament region explains the super toughness of rubber-modified semicrystalline polymers.

It has been observed that, at low test speeds, DBTT is independent of the interparticle distance in toughened PP[29] and PA6.[21] According to these studies, the dependence of the DBTT on interparticle distance can be established only at impact speeds when a significant temperature rise can be measured near the crack tip.[29] This effect, noted at low test speeds, cannot simply be associated with the fact that, at this rate of strain, the DBTT falls at a temperature lower than the glass transition of the dispersed phase, with a consequent rise of its cavitation resistance, because interparticle distance effects have also been shown in composites made of crystalline polymers and rigid fillers.[28]

Recently, a model has been proposed to take into account the additional contribution of the rubbery particles in the stabilization of dilatational bands.[30] Following this approach, during an impact test, the material below the fracture surface is in near adiabatic conditions.[12,26] The elastic potential energy released during crack propagation transforms into thermal energy which causes a strong heating of the material near the fracture surface. As a consequence, the yield stress decreases together with the energy absorbed during crack propagation. In these conditions, the crack tends to accelerate to such an extent that a very rapid crack propagation can occur, leading to a brittle fracture. The elastomeric particles can stabilize the growing crack by absorbing elastic energy, thus any increase in temperature will result in a parallel increase in elastic modulus and therefore elastic energy absorbed. It has been shown that the stabilizing effect of elastomeric particles is stronger when the interparticle distance, and the particle size, decreases.[30]

In the present contest, the VLDPE has such a low crystallinity that its mechanical behavior can be assimilated to that shown by a slightly crosslinked elastomer. In the case of the homopolymer blend, the average particle size is in the range 5–8 μm, whereas for the system PA6/VLDPE-*g*-DEM, the average size is approximately 1 μm. For the MA functionalized blends, the average particle size is approximately 0.2 μm. The lower particle size of these blends, compared with those functionalized with DEM, is in agreement with their lower DBTT. The PA6/VLDPE-*g*-MA blends also show a considerably higher resistance to crack propagation.

It is known that the particle size is related to the ratio between the melt viscosities of the two polymers during extrusion. When this ratio is near 1, a minimum particle size is obtained.[31] DEM has a lower reactivity respect to MA toward nylons and this might cause a lower level of interaction of the polyamide phase with VLDPE. As a consequence, a larger particle size is to be expected during extrusion. A different degree of re-

activity between the two functional groups can also be associated with a different morphology of the impact fracture surfaces of specimens of blends with VLDPE-*g*-MA and VLDPE-*g*-DEM, indicating that the MA functional groups leads to a stronger interface than DEM.

Unfortunately, in this work it was not possible to obtain materials with the same level of grafting of DEM and MA; therefore, a clear comparison between the two functional groups cannot be drawn. Further work will be necessary to compare materials with the same level of grafting and possibly the same particle size.

CONCLUSIONS

The results of the fracture and impact analysis show that the blends with compatibilized polyolefins display a very different behavior from that of the homopolymer blend. In fact, whereas the latter is fragile at all temperatures, the compatibilized blends show a DBTT that depends on the type of polyolefin functional group and test speed. Under impact conditions, the PA6/VLDPE-*g*-MA blend displays a lower DBTT (5°C) than the PA6/VLDPE-*g*-DEM blend (30°C). On the other hand, the maximum impact energy of the former blend is lower. The Nyltech blend shows a low DBTT and a high value of the maximum impact energy. The morphological analysis of the fracture surfaces of impact-tested specimens shows that cavitation phenomena are present in all ductile failures and the amount of cavitation seems to be related to the impact energy. In particular, it has been shown that blends with DEM, when tested in impact, show cavitation due to debonding at the interface, whereas blends with MA-grafted VLDPE show cavitation inside the particles.

The authors thank Dr. Speroni of Nyltech, Milano for providing materials and assisting with injection molding of the samples. The authors also thank Prof. A. J. Muller and A. M. Sanchez at the University Simon Bolivar in Caracas (Venezuela) for their contribution to the preparation of the functionalized polyethylene samples and their blends. The authors acknowledge the assistance of Mr. P. Narducci for the SEM analysis. This work was performed within the framework of the Agreement for Scientific Cooperation 1997–99 between CNR (Italy) and CONICIT (Venezuela).

REFERENCES

1. Xanthos, M. Reactive Extrusion, Properties and Practice; Hanser Publishers: Munich, 1992.
2. Keskkula, H.; Paul, D. R. In Nylon Plastics Handbook, Kohan, M., Ed.; Carl Hanser: Munich, 1994; Chapter 11.
3. van Duin, M.; Borggreve, R. J. M. In Reactive Modifiers for Polymers; Al-Malaika, S., Ed.; Chapman & Hall: London, 1997; pp. 133–162.
4. Cimmino, S.; D'Orazio, L.; Greco, R.; Maglio, G.; Malinconico, M.; Mancarella, C.; Martuscelli, E.; Palumbo, R.; Ragosta, G. Polym Eng Sci 1984, 25, 193.
5. Aglietto, M.; Benedetti, E.; Ruggeri, G.; Pracella, M.; d'Alessio, A.; Ciardelli, F. Macromol Symp 1995, 98, 1101.
6. Lambla, M.; Mestanza, R.; Seadan, M. Proceedings of the 4th European Symposium on Polymer Blends, Capri, Italy, May 24–26, 1993; p. 56.
7. Sun, Y.-J.; Hu, G.-H.; Lambla, M. Angew Makromol Chem 1995, 229, 1.
8. Gallucci, R. R.; Going, R. C. J Appl Polym Sci 1982, 27, 425.
9. Rosales, C.; Perera, R.; Ichazo, M.; Gonzales, J.; Rojas, H.; Sanchez, A.; Diaz-Barros, A. J Appl Polym Sci 1998, 70, 161.
10. Wu, S. Polymer 1985, 26, 1855.
11. Borggreve, R. J. M.; Gaymans, R. J. Polymer, 1989, 30, 63.
12. Dijkstra, K.; ter Laak, J.; Gaymans, R. J. Polymer 1994, 35, 1399.
13. Borggreve, R. J. M.; Gaymans, R. J.; Schuijer, J.; Ingen-Housz, J. F. Polymer 1985, 26, 1486.
14. Williams, J. G. Fracture Mechanics In The Physics of Glassy Polymers, 2nd Ed.; Haward, R. N.; Young, R. J., Eds.; Chapman & Hall: London, 1997.
15. Hale, G. A Testing Protocol for Conducting J Crack Growth Resistance Curve Tests in Plastics; ESIS, 1995.
16. ASTM D5045–93. Plane-Strain Toughness and Strain Energy Release Rate of Plastic Materials, 1993.
17. Wunderlich, B. Macromolecular Physics: Crystal Melting; Academic Press: New York, 1980; Vol. 3; Chapter 9.
18. Psarski, M.; Pracella, M.; Galeski, A. Polymer, to appear.
19. French, H.; Jungnickel, B. Colloid Polym Sci 1989, 16, 267.
20. Pracella, M.; Marin, E.; Magagnini, P. L.; Psarski, M., to appear.
21. Lazzeri, A. Toughening of Nylons; PhD Thesis, Cranfield University, UK, 1991.
22. Lazzeri, A.; Bucknall, C. B. J Mat Sci 1993, 28, 6799.
23. Dijkstra, K. Deformation and Fracture of Nylon 6: Rubber Blends, PhD Thesis, University of Twente, The Netherlands, 1993.
24. Muratoglu, O. K.; Argon, A. S.; Cohen, R. E.; Weinberg, M. Polymer 1995, 36, 921.

25. Muratoglu, O. K.; Argon, A. S.; Cohen, R. E. Polymer 1995, 36, 2143.
26. Muratoglu, O. K.; Argon, A. S.; Cohen, R. E.; Weinberg, M. Polymer 1995, 36, 4771.
27. Muratoglu, O. K.; Argon, A. S.; Cohen, R. E.; Weinberg, M. Polymer 1995, 36, 4787.
28. Argon, A. S.; Bartczak, Z.; Cohen, R. E.; Muratoglu, O. K. In Polymeric Composites: Expanding the Limits, Proceedings of the 18th Risø International Symposium on Materials Science; Andersen, S. I.; Brøndsted, P.; Lilholt, H.; Lystrup, Aa.; Rheinländer, J. T.; Sørensen, B. F.; Toftegaard, H., Eds.; Risø National Laboratory: Roskilde, Denmark, 1997.
29. van der Wal, A. The Fracture Behaviour of Polypropylene and Polypropylene-Rubber Blends, PhD Thesis, University of Twente, The Netherlands, 1996.
30. Lazzeri, A. The Kinetics of Dilatational Bands and the Interparticle Distance Effect in Rubber Toughened Polymers; 10th International Conference on Deformation, Yield and Fracture of Polymers, April 7–10, 1997, Cambridge, UK, p. 75.
31. Wu, S. Polym Eng Sci 1987, 27, 335.